

**Chest electrical impedance tomography examination, data analysis,
terminology, clinical use and recommendations: consensus statement of
the TRanslational EIT developmeNt stuDy group**

Inéz Frerichs, Marcelo B. P. Amato, Anton H. van Kaam, David G. Tingay, Zhanqi Zhao,
Bartłomiej Grychtol, Marc Bodenstein, Hervé Gagnon, Stephan H. Böhm, Eckhard Teschner,
Ola Stenqvist, Tommaso Mauri, Vinicius Torsani, Luigi Camporota, Andreas Schibler, Gerhard
K. Wolf, Diederik Gommers, Steffen Leonhardt, Andy Adler, TREND study group

ONLINE SUPPLEMENT 5

EIT measures

EIT measures

Overview

EIT measures are the values calculated from analysis of functional EIT (fEIT) images which are designed to represent different features of the lung function at level of the entire image (global measures) or large image regions. As described in EOS 4, an fEIT image is generated from a mathematical operation on a sequence of raw EIT images and the resulting EIT waveforms. Depending on the fEIT image type, a different aspect of physiological function is represented.

EIT measures are values derived from the examinations that are typically used to assess the present state of ventilation (and perfusion) distribution and trends. Thus, in contrast to an fEIT image, an EIT measure is a single parameter or small number of parameters which represent the physiological state. Images and numeric values are complementary. Figure E5.1 shows a schematic diagram of the relationship between the raw EIT image sequence, fEIT images, and EIT measures.

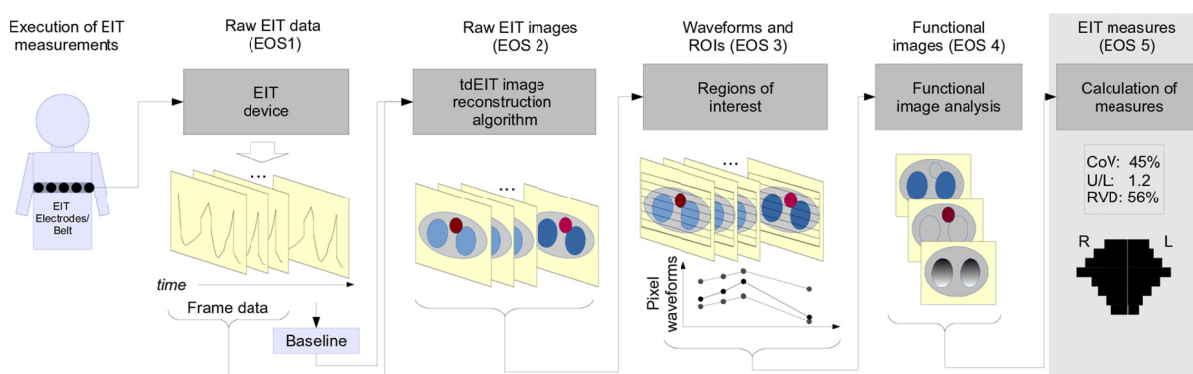


Figure E5.1. Schematic diagram of the calculation of EIT measures. First, from the raw EIT data (EOS 1), a sequence of EIT images is calculated (EOS 2). The time course of each image element (pixel) is analyzed to produce an fEIT image (EOS 4). From this fEIT image, further calculations are made to obtain EIT measures which each represent some aspect of the physiological state of the lung. Abbreviations: EOS, electronic online supplement; tdEIT, time-difference EIT; ROI, region-of-interest; CoV, center of ventilation; U/L, upper-to-lower ventilation ratio; RVD, regional ventilation delay; R, right; L, left.

Types of EIT measures

A large number of EIT measures have been proposed. To help categorize this work, EIT measures can be classified into three groups: averaged global or regional measures,

measures for characterization of spatial distribution of ventilation, and examination-specific measures.

1. *Average regional EIT measures* represent the functional measures used to generate fEIT images, only that the pixel values of these measures are averaged (or summed) in the whole image or its sections (e.g., quadrants or layers). For instance, pixel tidal impedance changes summed in all image pixels provide a global measure of regional tidal variation in the studied chest slice.

2. *Measures for characterization of the spatial distribution of ventilation* consist of measures which aim to describe the location and spatial configuration of the ventilated region. Examples are the center of ventilation and ventilation heterogeneity measures. These measures are also calculated from pixel functional measures.

3. *Examination-specific measures* characterize specific aspects of lung physiology using specific examinations or measurements of EIT in parallel with other signals, such as airway pressure. This is a varied group of EIT measures which is sometimes calculated from pixel functional measures, but can also be calculated using other approaches.

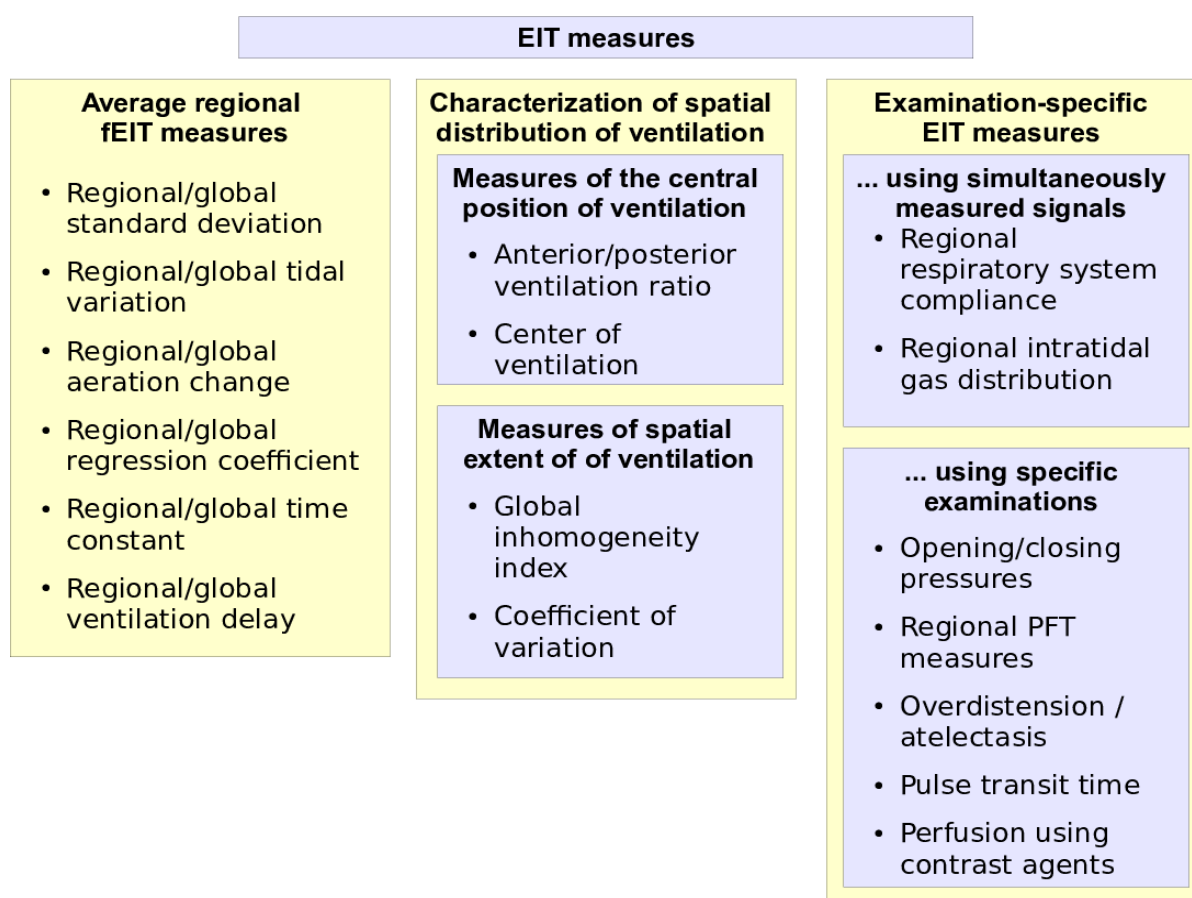


Figure E5.2. Classification of EIT measures into three principal groups, as well as the sub-classifications of the types of measures within each group. PFT, pulmonary function testing.

Average regional EIT measures

The first type of EIT measures are those representing the average (or sum) of fEIT measures. These measures are typically used to characterize the overall ventilation and aeration and the changes in these quantities, e.g. tidal volume, and changes in end-expiratory lung volume. Such EIT measures may be calculated in the whole image or in ROIs dividing the whole image into regions, as discussed in EOS 3. ROIs may be defined on the whole image or divide only the ventilated region identified as lungs.

In cases where the physiological effects of interest occur in the gravity direction and the patient is supine or prone, ROIs are defined to divide the defined region in the anteroposterior direction with horizontal divisions, into either two regions (an upper and lower region) or into a larger number of regions. The highest degree of spatial resolution offer the ventilation profiles calculated from the smallest layer ROIs with the height of one image pixel. A further division of ROIs is to consider a left/right division between image regions. These EIT measures allow description of physiological processes which differentially affect the left and right lungs. The most commonly used divisions have been into two (upper/lower divisions) or into four quadrant regions.

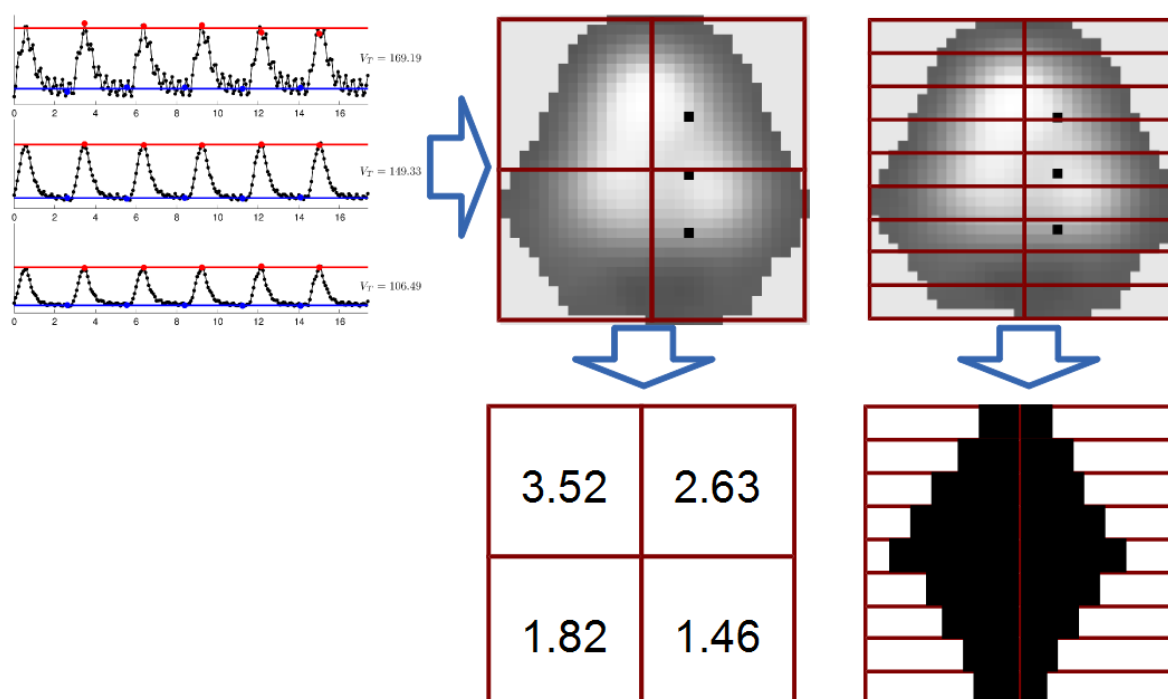


Figure E5.3. Illustration of the calculation of regional EIT measures, based on the tidal variation fEIT image of Figure E4.5 in EOS 4. Left: Regional EIT waveforms in three image pixels highlighted as small black squares in the images. Middle: Calculation of the average image values in each quadrant, where resulting values are shown in each quadrant, below. Right: Calculation of average image values in the left and right layers, resulting values are shown as the length of bars below.

The process of calculation of an average regional EIT measure is illustrated in figure E5.3, in which the tidal variation fEIT image is first calculated, and then the average pixel value in each quadrant is calculated and displayed. Such average (or summed) regional EIT measures may be applied to any of the fEIT images defined in EOS 4, as summarized in Table E5.1.

Table E5.1. EIT measures calculated from average (or summed) regional fEIT images.

EIT measure	fEIT image
Regional/global standard deviation EIT measure	Standard deviation fEIT image
Regional/global tidal variation EIT measure	Tidal variation fEIT image
Regional/global aeration change EIT measure	Aeration change fEIT image
Regional/global regression coefficient EIT measure	Regression coefficient fEIT image
Regional/global time constant EIT measure	Time constant fEIT image
Regional/global ventilation delay EIT measure	Ventilation delay fEIT image

Measures for characterizations of the spatial distribution of ventilation

The second group consists of measures aimed at characterizing the spatial distribution of ventilation in the image. Since a large part of the promise of EIT for ventilation monitoring is driven by its ability to calculate a regional map of ventilation, such measures are key to characterizing and summarizing this information.

As a descriptive statistical measure, the spatial distribution may be divided into measures as follows:

1. Measures of the central position of the distribution of ventilation
2. Measures of the spatial extent of the distribution of ventilation

Calculation of measures of the spatial distribution of ventilation requires using formulae which are more complicated than simply an average or sum of fEIT measures, and

are thus categorized as a different type of EIT measure. These types of measures are described below.

- **Measures of the central position of the distribution of ventilation**

Such measures globally characterize the orientation of the distribution of ventilation within the chest. The most common measures characterize the distribution in the anteroposterior direction. This direction is the clinically relevant when patients are examined in the supine or prone positions; i.e. it corresponds to the orientation of the gravity vector. However, when relevant to the physiology or the ventilation pattern, measures of right-left position have been used, such as for postural changes (1-3) or unilateral ventilation (4, 5).

- a. Anterior-to-posterior ventilation ratio (A/P ratio)***

A common measure of the anteroposterior distribution of ventilation is the anterior-to-posterior ventilation ratio (A/P ratio). This measure was originally called the "impedance ratio" (6). It has also been referred to as the upper-to-lower ventilation ratio (U/L ratio). As illustrated in Figure E5.4, this index relates the ventral impedance changes to dorsal impedance changes by computing

$$\text{A/P ratio} = (\text{Anterior ventilation}) / (\text{Posterior ventilation})$$

where the upper (ventral) and lower (dorsal) ventilation are calculated

$$(\text{Anterior ventilation}) = \text{Sum of pixel values in anterior half of image } (\Sigma A), \text{ and}$$

$$(\text{Posterior ventilation}) = \text{Sum of pixel values in posterior half of image } (\Sigma P).$$

The A/P ratio is thus the ratio between the sum of tidal impedance changes in the anterior and posterior halves of the functional image or the lung ROI within it, as illustrated in Figure E5.4. As the center of the distribution of ventilation moves ventrally, for instance during volume-controlled ventilation when positive end-expiratory pressure (PEEP) is decreased and dorsal atelectasis develops, the ventilation in the anterior region (ΣA) will increase, while the ventilation in the posterior region (ΣP) will decrease, resulting in an increase in A/P ratio.

While the A/P ratio is relatively widely used, we do not consider it to be the most robust measure of the vertical distribution of ventilation, and instead, recommend the center of ventilation (CoV), described below. Because A/P is a ratio, its value can become arbitrarily large if the posterior region (ΣP) has a low value. This means that the change in the A/P ratio is not proportional to the change in the position of ventilation. Additionally, the lung areas are not identical in the upper and lower halves of the image, which means that the A/P ratio is not expected to be equal to one, even in the case of uniform ventilation.

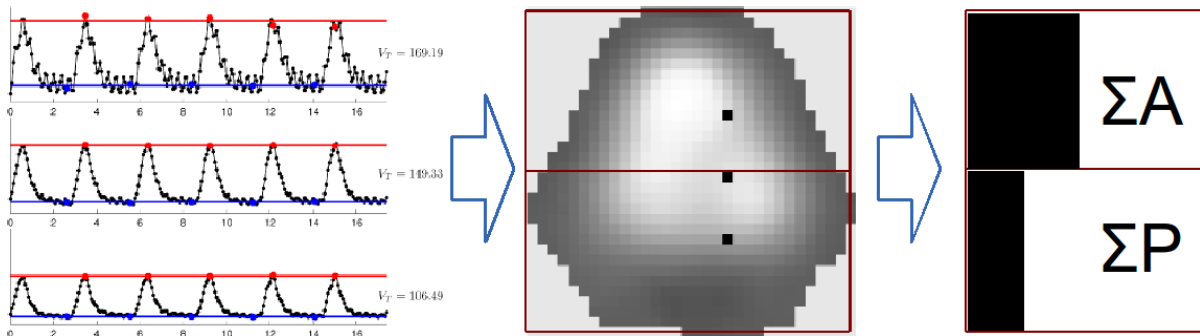


Figure E5.4. Illustration of computation of the anterior-to-posterior (A/P) ventilation ratio. The image is divided into two regions horizontally through the center, and the sum of the functional image values in the anterior (ΣA) and posterior (ΣP) areas are calculated.

b. Center of ventilation (CoV)

Another common measure of anteroposterior distribution is the center of ventilation (CoV), introduced by Frerichs et al. (7). The CoV is motivated by the concept of center of gravity (CoG) which is used in mechanics, defined as the location in space which characterizes the center of a distributed mass. (Indeed, the CoV parameter is sometimes called the CoG, although we do not recommend this terminology). CoV has been applied as a measure of ventilation distribution in several studies (8-12). For its application to an EIT image, the center of ventilation may be computed by

$$\text{CoV} [\%] = (\text{Height weighted pixel sum}) / (\text{Pixel sum})$$

where

$$(\text{Pixel sum}) = \sum (\Delta Z_j), \quad \text{and}$$

$$(\text{Height weighted pixel sum}) = \sum (y_j \times \Delta Z_j)$$

where y is the vertical position (y -axis) in the fEIT image, y_j is vertical position of pixel j and is scaled to increase in the gravity direction, and ΔZ_j is the image sum in the horizontal ROI at position y_j . The calculation of these values is illustrated in figure E5.5. CoV yields a value between 0 and 100% where 0% would indicate all image amplitude at the top, and 100% all amplitude at the bottom of the image. As the center of the distribution of ventilation moves dorsally, CoV increases. It is worth noting that a few authors have scaled the CoV differently (e.g. to scale it between -1 and $+1$ (13), or to reverse the direction such that 100% is the top (14)). For the horizontal axis, it is possible to define an analogous horizontal CoV, x_{CoV} .

The CoV has been used in many studies, as has been shown to be a sensitive index to describe opening and closing of the lung during incremental and decremental PEEP trials

(15). For many applications in which an EIT measure of the vertical position of ventilation is required, the CoV has been used in both experimental and clinical studies (8, 16-19). We recommend the use of CoV, instead of A/P ratio, since CoV is a linear measure of the position; thus a change in the position of the distribution of ventilation will introduce a proportional change in CoV, but not in the A/P ratio. Additionally, CoV is a function of each pixel layer in the image, and thus more sensitive than a simple division into upper and lower regions.

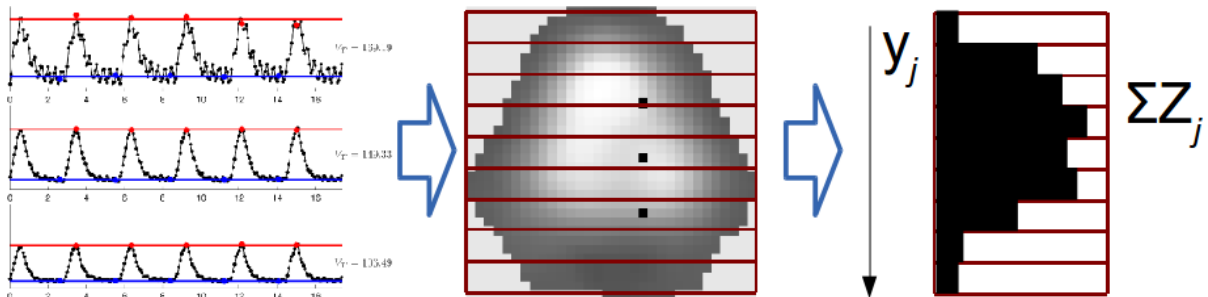


Figure E5.5. Illustration of computation of the center of ventilation (CoV). The image is divided into horizontal regions (of pixel width, thinner than illustrated). In each horizontal region, y_j , the image sum ΣZ_j is determined and the CoV calculated using the formula provided in the text above. Z , impedance.

- **Measures of the spatial extent of the distribution of ventilation**

These measures are designed to describe variations in the pattern of ventilation which are not simply a change in the position of the center of the distribution. Such characterizations are needed for several features of the image, depending on the physiology of interest.

The most common measures of this type are used to describe the overall degree of spatial heterogeneity of ventilation. For some applications, it is important to characterize the level of inhomogeneity in an EIT image, since many pathological processes compromise the more uniform distribution of ventilation which exists under normal conditions. Such measures are also calculated from the pixel functional measures. Examples are the global inhomogeneity index or the coefficient of variation.

a. Global inhomogeneity index

One characterization of the degree of inhomogeneity is the global inhomogeneity index (GI), introduced by Zhao et al. (20). The calculation of GI is based on the difference between

each pixel value and the median value of all pixels. These values are normalized by the sum of impedance values within the lung area.

$$GI = \Sigma(\text{pixel differences from median}) / \Sigma(\text{pixels})$$

where

$$\Sigma(\text{pixels}) = \Sigma (\Delta Z_j), \quad \text{and}$$

$$\Sigma(\text{pixel differences from median}) = \Sigma (\Delta Z_j - \Delta Z_{median})$$

where ΔZ_j is the fEIT image value in pixel j , ΔZ_{median} is the median image value, and all sums are calculated for all pixels j in the image. In (20-22), GI was based on the tidal variation fEIT image; however, the GI measure is applicable to other fEIT image types as well.

b. Coefficient of variation

The coefficient of variation (CV) is a statistical measure which characterizes the relative magnitude of the standard deviation of a distribution with respect to the distribution mean. Frerichs et al. (23) introduced the concept of using the CV to characterize the global heterogeneity in all image pixels. CV was defined for an fEIT image as

$$CV = SD (\text{fEIT}) / Mean (\text{fEIT})$$

where $SD (\text{fEIT})$ and $Mean (\text{fEIT})$ represent the standard deviation and mean of a given fEIT image across all image pixels.

In (23), CV was used to characterize the degree of ventilation heterogeneity during high-frequency oscillation ventilation when compared with conventional ventilation. In the study by Vogt et al. (24), CV was calculated from the fEIT pixel values of inspiratory vital capacity (IVC), forced expiratory volume in 1 s (FEV_1), forced vital capacity (FVC) and tidal variation. Based on these measures, an analysis was performed to determine the power of the EIT-based measures to discriminate between patients with obstructive pulmonary disease and healthy subjects.

Examination-specific EIT measures

These measures have been created in order to characterize a specific aspect of thoracic physiology, and require either specific examination procedures or measurements of EIT in parallel with other signals, such as airway pressure (or, in some cases, both). For convenience of description, we thus divide examination-specific EIT measures as follows:

1. EIT measures which require EIT recordings in parallel with other signals
2. EIT measures which require specific examination procedures.

Examples of the first type are regional respiratory system compliance or opening and closing pressure values, while an example of the second type are measures of pulse transit times. The types of measures are further described below.

- **EIT measures using simultaneously measured signals**

This subgroup consists of measures that are derived from the EIT data registered in parallel with other signals, mostly airway pressure. They aim at characterizing regional respiratory system mechanics, with the main focus on regional respiratory system compliance. The high EIT scan rates allow the assessment of intratidal changes in regional compliance. Another EIT measure of respiratory mechanics is the average regional respiratory time constant introduced by (25, 26), which is described above under "average regional EIT measures".

a. Regional respiratory system compliance

As described in EOS 4, an EIT-derived compliance fEIT image may be calculated, in which

$$C_j = \Delta Z_j / \Delta P$$

where C_j is a regional compliance value in an fEIT image pixel, ΔP is the change in pressure, typically measured at the airways opening, and ΔZ_j is the corresponding change in EIT image at pixel j . Regional compliance measures are averages or sums, or the maximum or minimum values within regions.

Regional EIT-derived values of compliance have predominantly been analyzed under dynamic conditions (12, 27-29), in which case the value of ΔP at the airway opening represents not only the effect of compliance, but also that of flow-resistive pressure. This means that a dynamic measurement of C_j is an underestimate of its true value. Several authors have studied respiratory system mechanics during quasi-static conditions identifying the landmark pressures at maximum compliance changes on the inflation (and sometimes also deflation) limbs of the low-flow pressure-volume maneuver (30-33). An EIT-based approach to determine regional respiratory system compliance in ventilated patients with spontaneous breathing activity using a short PEEP wave maneuver was described in (34).

b. Regional intratidal gas distribution

Regional intratidal gas distribution is an approach to characterize which parts of the lungs are filled at each stage of an inflation protocol. The goal of this EIT measure is to help identify intratidal regional recruitment and overdistention. To calculate regional intratidal gas distribution, the volume of gas (as reflected by the global impedance change) during

inflation is divided into a number of equal volume parts. During each volume part, the fraction of volume going into each lung ROI is calculated. These data are then graphed as the regional volume fraction vs. the inflation step.

Regional intratidal gas distribution was first introduced by Lowhagen et al. (29). In the original study, the authors divided inflation into eight steps and the lung into four horizontal ROIs. This work showed that the contribution of the dependent lung regions to the inspiration increases at higher PEEP levels. The same measure was used to assess the effect of different assist levels during pressure-support ventilation (PSV) and neurally-adjusted ventilatory assist (NAVA) on ventilation distribution (35), however, it was analyzed using only two (anterior and posterior) image layers. This measure was further used as a strategy to optimize PEEP settings in experimental (36) and clinical settings (16).

- **EIT measures using specific examinations**

- a. Regional pulmonary opening/closing pressures***

As described in EOS 4, the pixel opening and closing pressures can be calculated by detecting the time that the pixel waveform crosses a threshold. This approach was described by Pulletz et al. (37) and requires the use of a low-flow inflation and deflation maneuver. The fEIT image for each pixel is taken from the pressure at the time that the threshold is crossed. The use of a slow inflation and deflation means that pressures can be considered quasi-static, and that the opening and closing pressures reflect the physiological state of lung tissue without the flow-resistive effects. Based on the fEIT images of opening or closing pressures, regional average values can be calculated.

- b. Regional values of pulmonary function testing (PFT) measures***

During conventional pulmonary function testing using spirometry or whole body plethysmography, global lung function parameters like inspiratory vital capacity (IVC), forced expiratory volume in 1 s (FEV_1), forced vital capacity (FVC), FEV_1/FVC or mean maximum expiratory flow between 25 to 75% of FVC, are measured at the airways opening and used to assess the lung status of the patients. EIT enables the assessment of such measures on a regional basis by analysis of pixel EIT waveforms acquired during the examination of full inspiration from residual volume and subsequent forced full expiration. This approach has been used in a few studies to show the spatial and temporal heterogeneity of ventilation in patients with cystic fibrosis, chronic obstructive lung disease (COPD) or asthma (24, 38-42).

The EIT image pixel impedance values are proportional to expiratory volumes (43); thus, derivatives of pixel value can be considered proportional to expiratory flows. Without calibration, a direct comparison with spirometric parameters is not possible. To remove the requirement for calibration, ratios of maximum expiratory flows at 25% and 75% of vital capacity (MEF_{25}/MEF_{75}) during forced expiration were calculated for each pixel in lung regions in the EIT images (38, 39). This fEIT image was called the “regional obstruction map”; however, we propose the term “expiratory flow ratio fEIT image”. To create this image, MEF_{25}/MEF_{75} values are shown in each pixel of the image. Patients with obstructive lung diseases usually have a mean MEF_{25}/MEF_{75} value lower than 0.2 with high variations among pixels (39). Similar results have been observed for the regional EIT-derived FEV_1/FVC values (24, 41, 42). Healthy subjects had the highest values of pixel FEV_1/FVC with a narrow peak in the distribution histogram. The highest degree of heterogeneity with a flat distribution of the histogram of pixel values was noted in patients with COPD. The spatial distribution of pixel lung function measures of IVC, FEV_1 , FVC quantified as the coefficient of variation was also identified as most heterogeneous in these patients.

Another EIT measure based on PFT measures is based on the fEIT image of expiration times. This image is composed of pixel expiration times required to exhale certain amounts of volume of pixel FVC (e.g. 75%, denoted as t_{75}). These measures are effective to characterize the temporal distribution of regional lung ventilation (24, 41, 42). In COPD and asthma, delayed and more heterogeneous emptying than in the healthy lungs was noted.

c. Overdistension / Atelectasis [%]

As described in EOS 4, an image of regional overdistension and atelectasis/collapse may be calculated from analysis of a stepwise recruitment protocol (i.e. decremental PEEP trial after previous recruitment). The approach was defined by Costa et al. (44) and has been used also by (45), or a similar approach by (46). This approach classifies the fraction of overdistended or atelectatic units in each image pixel, $F(P)$, at each pressure level, P , as the fraction of maximum compliance of each pixel.

$$F(P) = 1 - C_{\text{dyn}}(P) / C_{\text{max}}$$

where $C_{\text{dyn}}(P)$ is the EIT-derived dynamic compliance and C_{max} is the maximum compliance seen at that pixel throughout the maneuver. An fEIT image pixel is classified as atelectatic if the current pressure P is below the one at which its maximum compliance occurs, while it is classified as overdistended in the converse case. This fEIT measure thus yields a fractional state of each image pixel. In order to calculate an EIT measure of global or regional

overdistension or atelectasis, the average value in the lung ROI (or an image region) is taken.

d. Measures of pulse transit time

Solà et al. defined a measure of pulse transit time from the region of the heart to the descending aorta (47). Pulse transit time measures are correlated with systemic blood pressure; however, typical measures use a peripheral site which means that the measure is modulated by vascular tone in the peripheral arteries, as well as other factors. In this work, the authors demonstrated that EIT is able to measure pulse transit time centrally, in a location (the aorta) where no modulation by vascular tone occurs. First, ROIs are identified corresponding to the heart and aorta, and in the EIT raw image sequence, pixel waveforms are calculated for these ROIs. The pulse transit time is then the time difference between the cardiac pulse in the waveform in the aortic ROI compared to that in the heart region. Because the aortic region is small, its signal is relatively weak. In order to improve the robustness of the measure, the average pulse transit time in the EIT waveform was calculated by robust parametric detection algorithm. This work showed a strong correlation between EIT measures of pulse transit time, and arterial blood pressure measurements in an experimental animal.

e. Measures of perfusion with contrast agents

Cardiac output and pulmonary blood flow represent important physiological parameters with clinical significance for patient management. As discussed in EOS 4, EIT signals contain a pulsatility component, which is associated with the contribution of blood flow at the cardiac rate to the EIT signals. The pulsatility gives useful information on the perfusion, but can deviate from it for several reasons (see EOS 4).

In order to obtain more accurate measures of regional lung perfusion, it is necessary to use EIT contrast agents. This approach was initially proposed by Frerichs et al. (48), in which a bolus of hypertonic saline was administered to visualize blood flow through lung regions. In the original work boli of 15 or 20ml of 5.85% NaCl were injected through the proximal or distal openings of a Swan-Ganz catheter. Figure E5.6 shows the EIT waveforms in two pixels following a saline bolus. There is a clear delay between the signal in the heart and lungs due to the propagation time through the pulmonary arteries.

Additional work with contrast agent-based perfusion measures was done by Borges et al. (49). Since the electrical conductivity of fluid is determined by the ionic concentration, hypertonic saline will increase the conductivity and thus be visible in the raw EIT images

(50). Some work to consider other contrast agents, such as temperature decreases or sucrose solutions (which decrease conductivity) has not been successful (51). While such images offer extremely useful information, their utility is limited by the relative invasiveness of the procedure. It is possible only in patients who already have a central catheter, and can be repeated only as often as is safe considering the effects of the additional saline on the patient.

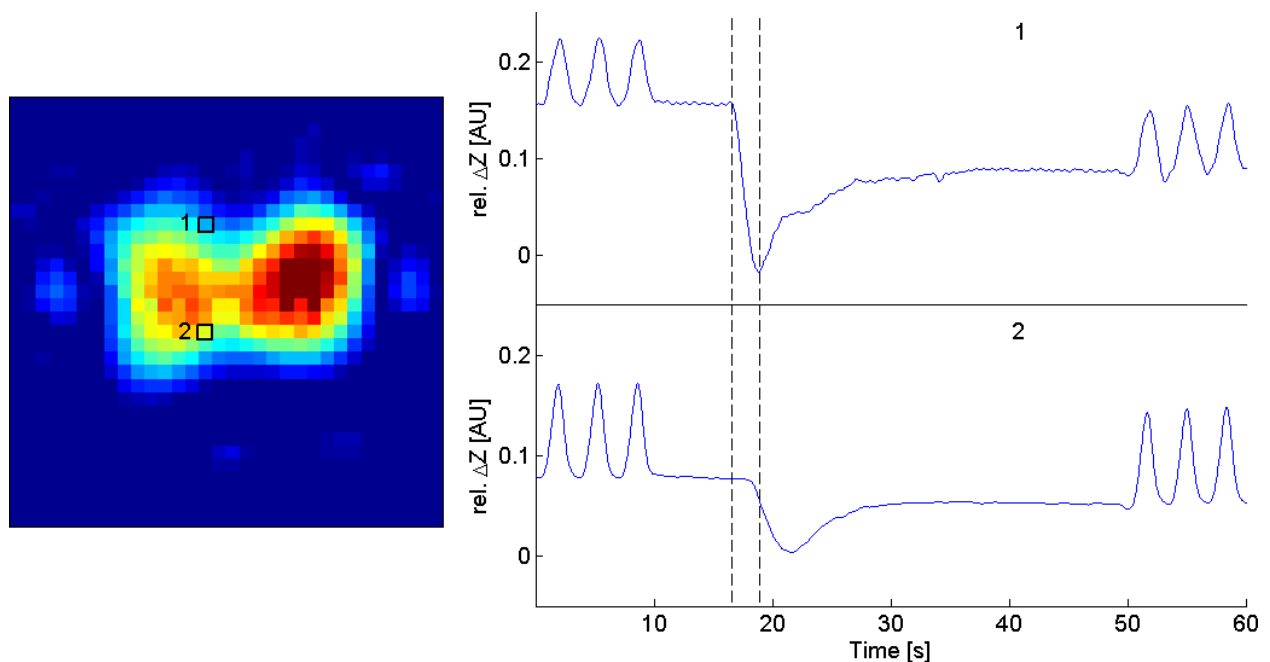


Figure E5.6. Regional EIT waveforms obtained in one pixel located in the anterior heart and posterior lung region following a bolus injection of 10% NaCl solution via a central venous line. The location of the pixels is indicated in the fEIT standard deviation image (left) with small squares and waveform numbers. The data were obtained in a mechanically ventilated supine pig using the Goe-MF II EIT device (CareFusion, Höchberg, Germany) before and after a breath-hold and bolus injection (52). The waveforms show the regional fall in impedance resulting from the passage of electrically conductive saline through the heart and vessels. Note the earlier onset of in the heart waveform as compared to the posterior lung. The dashed lines visualize the time delay.

Document preparation

The first draft of this online document was prepared by A. Adler with collaboration of I. Frerichs, Z. Zhao, B. Grychtol, S. Leonhardt and D. Gommers. It was reviewed and approved by all other authors and collaborators.

References

1. Frerichs I, Dudykevych T, Hinz J, Bodenstein M, Hahn G, Hellige G. Gravity effects on regional lung ventilation determined by functional EIT during parabolic flights. *J Appl Physiol* 2001;91:39-50.
2. Heinrich S, Schiffmann H, Frerichs A, Klockgether-Radke A, Frerichs I. Body and head position effects on regional lung ventilation in infants: An electrical impedance tomography study. *Intensive Care Med* 2006;32:1392-1398.
3. Schnidrig S, Casaulta C, Schibler A, Riedel T. Influence of end-expiratory level and tidal volume on gravitational ventilation distribution during tidal breathing in healthy adults. *Eur J Appl Physiol* 2013;113:591-598.
4. Pulletz S, Elke G, Zick G, Schadler D, Scholz J, Weiler N, Frerichs I. Performance of electrical impedance tomography in detecting regional tidal volumes during one-lung ventilation. *Acta Anaesthesiol Scand* 2008;52:1131-1139.
5. Steinmann D, Stahl CA, Minner J, Schumann S, Loop T, Kirschbaum A, Priebe HJ, Guttman J. Electrical impedance tomography to confirm correct placement of double-lumen tube: A feasibility study. *Br J Anaesth* 2008;101:411-418.
6. Kunst PW, Vazquez de Anda G, Bohm SH, Faes TJ, Lachmann B, Postmus PE, de Vries PM. Monitoring of recruitment and derecruitment by electrical impedance tomography in a model of acute lung injury. *Crit Care Med* 2000;28:3891-3895.
7. Frerichs I, Hahn G, Golisch W, Kurpitz M, Burchardi H, Hellige G. Monitoring perioperative changes in distribution of pulmonary ventilation by functional electrical impedance tomography. *Acta Anaesthesiol Scand* 1998;42:721-726.
8. Frerichs I, Dargaville PA, van Genderingen H, Morel DR, Rimensberger PC. Lung volume recruitment after surfactant administration modifies spatial distribution of ventilation. *Am J Respir Crit Care Med* 2006;174:772-779.
9. Schibler A, Yuill M, Parsley C, Pham T, Gilshenan K, Dakin C. Regional ventilation distribution in non-sedated spontaneously breathing newborns and adults is not different. *Pediatr Pulmonol* 2009;44:851-858.
10. Miedema M, de Jongh FH, Frerichs I, van Veenendaal MB, van Kaam AH. Changes in lung volume and ventilation during surfactant treatment in ventilated preterm infants. *Am J Respir Crit Care Med* 2011;184:100-105.
11. Karsten J, Luepschen H, Grossherr M, Bruch HP, Leonhardt S, Gehring H, Meier T. Effect of PEEP on regional ventilation during laparoscopic surgery monitored by electrical impedance tomography. *Acta Anaesthesiol Scand* 2011;55:878-886.

12. Bikker IG, Preis C, Egal M, Bakker J, Gommers D. Electrical impedance tomography measured at two thoracic levels can visualize the ventilation distribution changes at the bedside during a decremental positive end-expiratory lung pressure trial. *Crit Care* 2011;15:R193.
13. Wolf GK, Grychtol B, Frerichs I, Zurakowski D, Arnold JH. Regional lung volume changes during high-frequency oscillatory ventilation. *Pediatr Crit Care Med* 2010;11:610-615.
14. Radke OC, Schneider T, Heller AR, Koch T. Spontaneous breathing during general anesthesia prevents the ventral redistribution of ventilation as detected by electrical impedance tomography: A randomized trial. *Anesthesiology* 2012;116:1227-1234.
15. Luepschen H, Meier T, Grossherr M, Leibecke T, Karsten J, Leonhardt S. Protective ventilation using electrical impedance tomography. *Physiol Meas* 2007;28:S247-260.
16. Blankman P, Hasan D, Groot Jebbink E, Gommers D. Detection of 'best' positive end-expiratory pressure derived from electrical impedance tomography parameters during a decremental positive end-expiratory pressure trial. *Crit Care* 2014;18:R95.
17. Tingay DG, Wallace MJ, Bhatia R, Schmolzer GM, Zahra VA, Dolan MJ, Hooper SB, Davis PG. Surfactant before the first inflation at birth improves spatial distribution of ventilation and reduces lung injury in preterm lambs. *J Appl Physiol* 2014;116:251-258.
18. Pham TM, Yuill M, Dakin C, Schibler A. Regional ventilation distribution in the first 6 months of life. *Eur Respir J* 2011;37:919-924.
19. Rooney D, Friese M, Fraser JF, K RD, Schibler A. Gravity-dependent ventilation distribution in rats measured with electrical impedance tomography. *Physiol Meas* 2009;30:1075-1085.
20. Zhao Z, Moller K, Steinmann D, Frerichs I, Guttman J. Evaluation of an electrical impedance tomography-based global inhomogeneity index for pulmonary ventilation distribution. *Intensive Care Med* 2009;35:1900-1906.
21. Zhao Z, Steinmann D, Frerichs I, Guttman J, Moller K. PEEP titration guided by ventilation homogeneity: A feasibility study using electrical impedance tomography. *Crit Care* 2010;14:R8.
22. Becher T, Kott M, Schädler D, Vogt B, Meinel T, Weiler N, Frerichs I. Influence of tidal volume on ventilation inhomogeneity assessed by electrical impedance tomography during controlled mechanical ventilation. *Physiol Meas* 2015;36:1137-1146.
23. Frerichs I, Achtzehn U, Pechmann A, Pulletz S, Schmidt EW, Quintel M, Weiler N. High-frequency oscillatory ventilation in patients with acute exacerbation of chronic obstructive pulmonary disease. *J Crit Care* 2012;27:172-181.

24. Vogt B, Pulletz S, Elke G, Zhao Z, Zabel P, Weiler N, Frerichs I. Spatial and temporal heterogeneity of regional lung ventilation determined by electrical impedance tomography during pulmonary function testing. *J Appl Physiol* 2012;113:1154-1161.
25. Miedema M, de Jongh FH, Frerichs I, van Veenendaal MB, van Kaam AH. Regional respiratory time constants during lung recruitment in high-frequency oscillatory ventilated preterm infants. *Intensive Care Med* 2012;38:294-299.
26. Pulletz S, Kott M, Elke G, Schadler D, Vogt B, Weiler N, Frerichs I. Dynamics of regional lung aeration determined by electrical impedance tomography in patients with acute respiratory distress syndrome. *Multidiscip Respir Med* 2012;7:44.
27. Dargaville PA, Rimensberger PC, Frerichs I. Regional tidal ventilation and compliance during a stepwise vital capacity manoeuvre. *Intensive Care Med* 2010;36:1953-1961.
28. Zick G, Elke G, Becher T, Schadler D, Pulletz S, Freitag-Wolf S, Weiler N, Frerichs I. Effect of PEEP and tidal volume on ventilation distribution and end-expiratory lung volume: A prospective experimental animal and pilot clinical study. *PLoS One* 2013;8:e72675.
29. Lowhagen K, Lundin S, Stenqvist O. Regional intratidal gas distribution in acute lung injury and acute respiratory distress syndrome-assessed by electric impedance tomography. *Minerva Anesthesiol* 2010;76:1024-1035.
30. van Genderingen HR, van Vught AJ, Jansen JR. Estimation of regional lung volume changes by electrical impedance pressures tomography during a pressure-volume maneuver. *Intensive Care Med* 2003;29:233-240.
31. Frerichs I, Dargaville PA, Rimensberger PC. Regional respiratory inflation and deflation pressure-volume curves determined by electrical impedance tomography. *Physiol Meas* 2013;34:567-577.
32. Grychtol B, Wolf GK, Arnold JH. Differences in regional pulmonary pressure-impedance curves before and after lung injury assessed with a novel algorithm. *Physiol Meas* 2009;30:S137-148.
33. Hinz J, Moerer O, Neumann P, Dudykevych T, Frerichs I, Hellige G, Quintel M. Regional pulmonary pressure volume curves in mechanically ventilated patients with acute respiratory failure measured by electrical impedance tomography. *Acta Anaesthesiol Scand* 2006;50:331-339.
34. Becher TH, Bui S, Zick G, Blaser D, Schadler D, Weiler N, Frerichs I. Assessment of respiratory system compliance with electrical impedance tomography using a positive end-expiratory pressure wave maneuver during pressure support ventilation: A pilot clinical study. *Crit Care* 2014;18:679.

35. Blankman P, Hasan D, van Mourik MS, Gommers D. Ventilation distribution measured with EIT at varying levels of pressure support and neurally adjusted ventilatory assist in patients with ali. *Intensive Care Med* 2013;39:1057-1062.
36. Bikker IG, Blankman P, Specht P, Bakker J, Gommers D. Global and regional parameters to visualize the 'best' PEEP during a peep trial in a porcine model with and without acute lung injury. *Minerva Anesthesiol* 2013;79:983-992.
37. Pulletz S, Adler A, Kott M, Elke G, Gawelczyk B, Schadler D, Zick G, Weiler N, Frerichs I. Regional lung opening and closing pressures in patients with acute lung injury. *J Crit Care* 2012;27:323 e311-328.
38. Zhao Z, Fischer R, Frerichs I, Muller-Lisse U, Moller K. Regional ventilation in cystic fibrosis measured by electrical impedance tomography. *J Cyst Fibros* 2012;11:412-418.
39. Zhao Z, Muller-Lisse U, Frerichs I, Fischer R, Moller K. Regional airway obstruction in cystic fibrosis determined by electrical impedance tomography in comparison with high resolution CT. *Physiol Meas* 2013;34:N107-114.
40. Vogt B, Elke G, von Bismarck P, Ankermann T, Weiler N, Frerichs I. Regional pulmonary function testing by electrical impedance tomography in healthy children and children with asthma. *Eur Respir J* 2012;40 Suppl. 56:3296.
41. Frerichs I, Zhao Z, Becher T, Zabel P, Weiler N, Vogt B. Regional lung function determined by electrical impedance tomography during bronchodilator reversibility testing in patients with asthma. *Physiol Meas* 2016;37:698-712.
42. Vogt B, Zhao Z, Zabel P, Weiler N, Frerichs I. Regional lung response to bronchodilator reversibility testing determined by electrical impedance tomography in chronic obstructive pulmonary disease. *Am J Physiol Lung Cell Mol Physiol* 2016;311:L8-L19.
43. Marquis F, Coulombe N, Costa R, Gagnon H, Guardo R, Skrobik Y. Electrical impedance tomography's correlation to lung volume is not influenced by anthropometric parameters. *J Clin Monit Comput* 2006;20:201-207.
44. Costa EL, Borges JB, Melo A, Suarez-Sipmann F, Toufen C, Jr., Bohm SH, Amato MB. Bedside estimation of recruitable alveolar collapse and hyperdistension by electrical impedance tomography. *Intensive Care Med* 2009;35:1132-1137.
45. Gomez-Laberge C, Arnold JH, Wolf GK. A unified approach for EIT imaging of regional overdistension and atelectasis in acute lung injury. *IEEE Trans Med Imaging* 2012;31:834-842.
46. Grychtol B, Wolf GK, Adler A, Arnold JH. Towards lung EIT image segmentation: Automatic classification of lung tissue state from analysis of EIT monitored recruitment manoeuvres. *Physiol Meas* 2010;31:S31-43.

47. Sola J, Adler A, Santos A, Tusman G, Sipmann FS, Bohm SH. Non-invasive monitoring of central blood pressure by electrical impedance tomography: First experimental evidence. *Med Biol Eng Comput* 2011;49:409-415.
48. Frerichs I, Hinz J, Herrmann P, Weisser G, Hahn G, Quintel M, Hellige G. Regional lung perfusion as determined by electrical impedance tomography in comparison with electron beam CT imaging. *IEEE Trans Med Imaging* 2002;21:646-652.
49. Borges JB, Suarez-Sipmann F, Bohm SH, Tusman G, Melo A, Maripuu E, Sandstrom M, Park M, Costa EL, Hedenstierna G, Amato M. Regional lung perfusion estimated by electrical impedance tomography in a piglet model of lung collapse. *J Appl Physiol* 2012;112:225-236.
50. Brown BH, Leathard A, Sinton A, McArdle FJ, Smith RW, Barber DC. Blood flow imaging using electrical impedance tomography. *Clin Phys Physiol Meas* 1992;13 Suppl A:175-179.
51. Mamatjan Y, Grychtol B, Gaggero P, Justiz J, Koch VM, Adler A. Evaluation and real-time monitoring of data quality in electrical impedance tomography. *IEEE Trans Med Imaging* 2013;32:1997-2005.
52. Elke G, Hintze C, Meybohm P, Biederer J, Weiler N, Frerichs I. Regional lung perfusion measured by electrical impedance tomography – a comparison of the bolus contrast and frequency-filtering approaches. *Am J Respir Crit Care Med* 2013;187:A1531.